High sensitivity deflection detection of nanowires

Babak Sanii and Paul Ashby
Molecular Foundry, LBNL, Berkeley, CA 94618, USA
(Dated: 28 October 2009)

A critical limitation of Nano-electromechanical systems (NEMS) is the lack of a high sensitivity position detection mechanism. We introduce a non-interferometric optical approach to determine the position of nanowires with high sensitivity and bandwidth. Its physical origins and limitations are determined by Mie scattering analysis. This enables a dramatic miniaturization of detectable cantilevers, with attendant reductions to the fundamental minimum force noise in highly damping environments. We measure the force-noise of an 80nm radius Ag_2Ga nanowire-cantilever in water at 1.9 $fN/\sqrt{Hz}$.

PACS numbers:

Micromechanical force sensors have transformed scientific metrology due to their high force sensitivity, with the most ubiquitous example being the multiple variants of atomic force microscopy. The high force sensitivity is due to the small size of the device reducing energy dissipation and the resulting thermal force fluctuations[1]. Typical microcantilever based force sensors are 60-500 μm long, 25-40 μm wide and 0.2-8 μm thick. Diminishing the cantilever dimensions to the nanoscale is appealing for further increasing force sensitivity[2]. While procedures to manufacture nano-cantilevers exist[3–5] the detection mechanism is the limiting factor in many applications, especially in viscous environments.

Conventionally, the deflection of a microcantilever is measured by a change in the reflected angle of an incident laser, as measured by a split photodetector. The optimal design requires a flat surface on the cantilever sufficiently large so as to produce a specular reflection, and the signal quality drops off significantly as the number of backscattered photons decreases[6, 7].

Here we present a simple optical detection scheme that discerns the position of a nano-cantilever with high sensitivity and bandwidth. The scheme places the nanowire near the focus of a laser polarized parallel to the length of the wire[5]. The forward light pattern is incident on a split photodiode, and its difference signal is used to measure the position of the nanowire with respect to the laser focus. The system is compatible with ambient pressure and liquid-submerged environments, and does not require an interferometric optical path.

We adapt Mie scattering analysis to establish that the difference signal of a split photodiode can be used as a high-sensitivity measure of the nanowire's position. We approximate the incident electromagnetic wave as a converging Gaussian beam, and the nanowire as a conducting cylinder. These approximations allow us to determine a series solution of our detection scheme's output.

The analytical approach, adapted from Kozaki[8], consists of two steps. First, the incident beam is expressed in cylindrical coordinates as a series with coefficients determined from its Gaussian initial conditions. Second, the scattered light is expressed in coefficients that are determined by the boundary condition of a vanishing tangential electric field at the surface of the conducting nanowire.

To express the incident Gaussian beam's electric field (E) in cylindrical coordinates we begin by taking the Fourier transform ($E(y) \Rightarrow \hat{E}(\alpha)$, α is the spatial frequency) of the wave equation ($\frac{\partial^2 E}{\partial y^2} + \frac{\partial^2 E}{\partial z^2} + k_o^2 E = 0$, $k_o = \frac{2\pi}{\lambda}$, λ is the wavelength of the incident light) and solve the resulting differential equation with respect to z (see Fig 1Ai for the coordinate system). We impose initial conditions of a Gaussian with a $\frac{1}{e}$ half-width of w_o and an offset from the center of the cylinder in the y-axis of y_o. For convenience, the physical parameters of the system are noted by red colored text in the analysis. An inverse Fourier transform retrieves the real-space incident electric field, E^{inc}:

$$E^{inc} = \frac{1}{2\pi}\int_{-\infty}^{\infty} \mathcal{FT}(e^{-\frac{(y-y_o)^2}{{w_o}^2}}) e^{iz\sqrt{{k_o}^2-\alpha^2}} e^{-i\alpha y} d\alpha \quad (1)$$

$$E^{inc} = \frac{w_o}{2\sqrt{\pi}}\int_{-\infty}^{\infty} e^{-\frac{\alpha^2 {w_o}^2}{4} - i\alpha y_o - i(z\sqrt{{k_o}^2-\alpha^2}+\alpha y)} d\alpha \quad (2)$$

This expression is converted into cylindrical coordinates ($z = \rho cos(\theta)$, $y = \rho sin(\theta)$, $\alpha \equiv k_o sin(\gamma)$) and trigonometric identities are used to reformulate the imaginary portion of the exponent of Eqn. 2 to the plane wave expansion as follows

$$e^{-i(z\sqrt{{k_o}^2-\alpha^2}+\alpha y)} = e^{-ik_o\rho cos(\theta-\gamma)} \quad (3)$$

$$= \sum_{n=-\infty}^{\infty} i^{-n} e^{in(\theta-\gamma)} J_n(k_o\rho) \quad (4)$$

Substituting Eqn. 4 into 2 produces the expression for an incident electric field with Gaussian initial conditions, in cylindrical coordinates:

$$E^{inc} = \sum_{n=-\infty}^{\infty} i^{-n} e^{in\theta} J_n(k_o\rho) A_n \quad (5)$$

$$A_n = \frac{w_o}{2\sqrt{\pi}}\int_{-\infty}^{\infty} e^{-\frac{\alpha^2 {w_o}^2}{4} - in\sin^{-1}(\frac{\alpha}{k_o}) - iy_o\alpha} d\alpha \quad (6)$$

The scattered electric field (E^{scat})is represented similarly, but with as yet undetermined coefficients (B_n) and a Hankel function of the 2nd kind ($H_n^{(2)}$) instead of a Bessel function (J_n)[9].

$$E^{scat} = \sum_{n=-\infty}^{\infty} i^{-n} e^{in(\theta)} H_n^{(2)}(k_o\rho) B_n \tag{7}$$

B_n is determined by imposing a boundary condition such that the sum of E^{scat} and E^{inc} vanishes on the surface of the conducting nanowire (i.e., when ρ is the radius of the nanowire, ρ_o).

$$B_n = -\frac{J_n(k_o\rho_o)}{H_n^{(2)}(k_o\rho_o)} A_n \tag{8}$$

The first 180 terms of Eqns. 5-8 are calculated, the electric fields added and the result squared to determine the expected signal on a far field detector (Using Matlab, Mathworks). The integral in equation 6 is intractable; earlier analysis solved the integral by approximating both $sin^{-1}(\alpha/k_o)$ and $\sqrt{k_o^2 - \alpha^2}$ with the first two terms of their respective Taylor series[8, 10]. However, these approximations are only valid when the wavelength is much smaller than the half-spotsize. Here we approximate the integral's value using Gauss/Lobatto quadrature[11] and limit the integration such that $sin^{-1}(\alpha/k_o)$ is real, to avoid branch cut discontinuities.

Within the collecting optic's numerical aperture (0.45), each half of the angular distribution is summed, and the reported signal is the difference between the left and the right sums. The analysis was repeated for a range of displacements between the center of the Gaussian beam's focus and the nanowire (see 1A), as well as a range of nanowire and laser focus sizes. The simulated split-photodiode's difference signal as a function of the separation between the cylinder and the beam focus (e.g., Fig 1B) reveals a characteristic profile reminiscent of profiles of beads translated through the focus of an optical trap[12]. The steepest slope of this profile corresponds to the region of greatest sensitivity. We find that for a 632.8nm wavelength beam and a conductive cylindrical material in air, both the size of the cylinder and the size of the focussed beam significantly affect the system's sensitivity. We find comparable relationships for nanowires immersed in water (see SI).

The relative sensitivity-to-noise ratio does not appear to increase monotonically with diminished cylinder and laser focus sizes. Instead several domains of enhanced sensitivity are observed. In the range of sizes shown in Fig 1C we observe two local maxima clustered around $\approx 500nm$ spot-sizes, with the most prominent one occurring when the nanowire's radius is $\approx 120nm$. This sensitivity to noise maximum occurs as the nanowire is in the middle of the laser beam, and is a result of competing effects. Nanowires significantly smaller than the spotsize produce less of a relative disturbance in the transmitted light, and nanowires larger than the spotsize preclude the formation of the position-sensitive split-forward lobes seen in Fig 1Aiii. Close inspection of the other local maximum, centered around $\approx 500nm$ radii nanowires, reveals that for this region the steepest slope of the position vs. split-photodiode difference signal graph is not where the nanowire is in the middle of the beam. Rather it occurs as the occluding nanowire exits the beam.

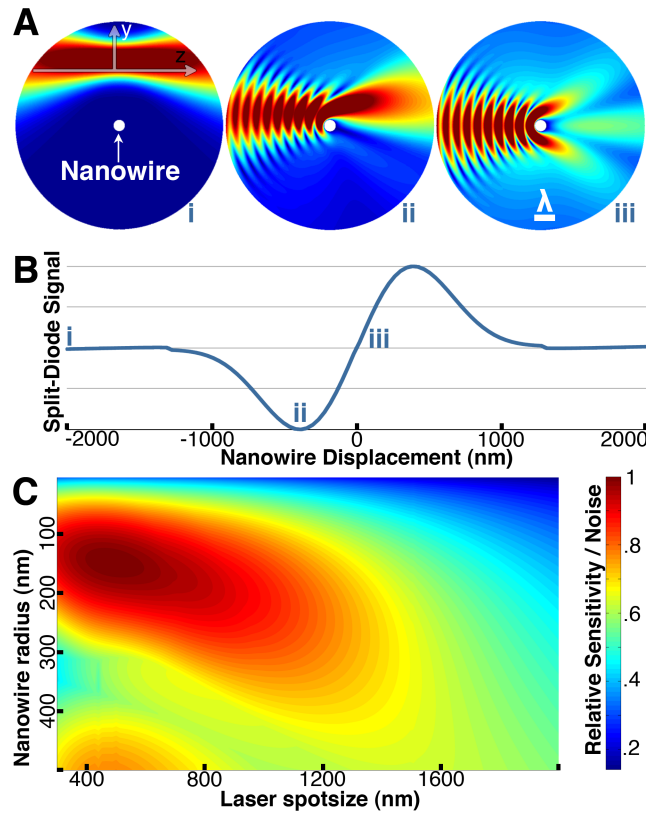

FIG. 1: A: The calculated local intensity as a 166nm radius nanowire translates across the focus of a 632.8nm wavelength Gaussian beam with a $1/e$ full width of $\approx 1044nm$, in air. B: The profile of the simulated signal on the split-photodiode as the nanowire in A is translated across the beam, in normalized ordinate units. The spot-nanowire separations shown in A are marked with Roman numerals. C: A map of the sensitivity to shot-noise ratio of the detection scheme as a function of 1/e spot diameter (150 samples, 200-2000nm) and nanowire radius (150 samples, 25-500nm), normalized and interpolated linearly between samples. Sensitivity is defined as the steepest slope of the calculated translation profile, and the relative shot-noise is approximated by the square root of the total power incident on the split photodiode, accounting for backscattering losses from the nanowire.

This analysis allows us to consider whether the detection scheme should use light that scatters forwards or backwards from nanowires for position sensing[5, 13]. The ratio of forwards to backward sensitivity reveals that forward scattering is preferred for most nanowires, with the exception of nanowire/spotsize combinations where the nanowire occludes the beam (e.g., near the large

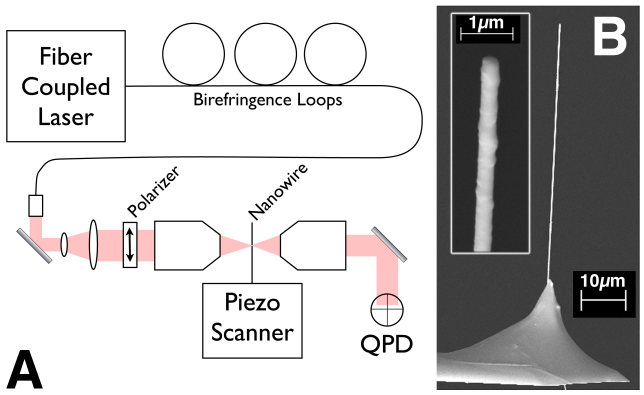

FIG. 2: A: Optical layout of the detection scheme. B: Scanning Electron Microscopy (SEM) image of a representative Ag_2Ga nanowire, with a magnified inset of the tip. This nanowire is $59\mu m$ long, with a radius of $166nm$.

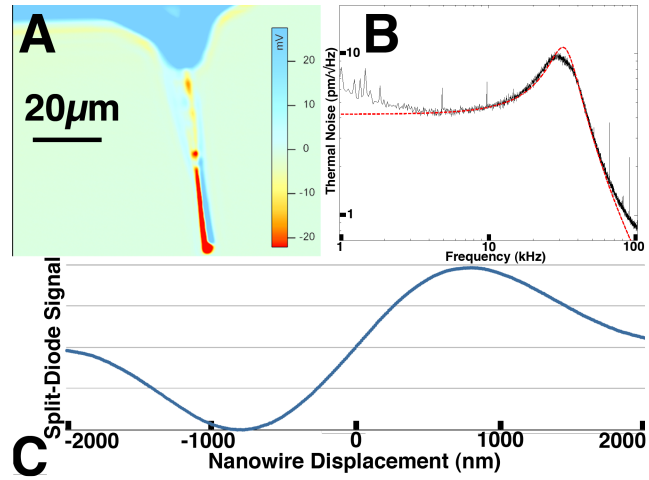

FIG. 3: A: Map of the photodiode's difference signal as the nanowire shown in Fig. 2B is laterally scanned through the laser beam. B: The measured thermal fluctuation spectrum of the nanowire, in air. Here the focussing objective's N.A. was 0.95. The dashed red line is the predicted thermal fluctuation spectrum from viscous fluid model[15] of the nanowire in air . C: A profile of the detected split-photodiode signal as the nanowire is translated across the beam. The spotsize used in measuring this profile was $\approx 1044nm$.

nanowire, small spot-size region discussed above). For sub-micron nanowires, forward scattering is most preferred when the spotsize is $1.38\mu m$ and the nanowire radius is 90nm; here forward scattering produces a better sensitivity-to-noise metric by a factor of 2.32 (see SI).

Experimentally, the optical design (see Fig 2A) requires polarization control and fine positioning of the nanowire in the focus of the beam. The laser source (Melles Griot 632.8nm, 5mW or CrystalLaser 785nm, 120mW) is coupled to a single-mode fiber that is looped three times to introduce birefringence, and each loop is twisted to tune the polarization of the transmitted light. The fiber output is collimated, expanded, re-polarized and fed into a microscope objective (Nikon 40x or 100x) that focuses it on the nanowire. The nanowire is positioned in the laser beam by a two dimensional piezoelectric scan stage (Thorlabs). The resulting forward light pattern is collected by a second objective (Nikon 20x), and steered onto a quadrant-photodiode module (Pacific Silicon Sensor). The working distance between the objectives was greater than a cm, sufficiently large enough for a wet cell with planar glass walls to fit. A controller (Asylum Research) drives the piezo stage, and monitors the difference and sum signals from the quad-photodiode. Nanowires primarily used in this study were bought commercially (Nauganeedles Inc.) and consist of Ag_2Ga crystals grown off of stiff ($40N/m$) AFM cantilevers[14] (e.g., see Fig 2B).

The difference in voltage between the halves of the photodiode (across the axis of the nanowire) is used to infer the nanowire's lateral position with respect to the focus of the laser spot. A map of the nanowire's difference signal as a function its position in the beam is shown in Fig 3A. A typical trace of the difference signal as a function of the nanowires position with respect to the beam is shown in Fig 3C. In this case, the region of greatest sensitivity is when the nanowire is near focus of the beam, where the signal from the split-photodiode changes linearly for several hungred nm with nanowire displacement. The linear relationship in this region allows a single scaling constant, with units of meters per volt, to characterize the sensitivity of the system.

While the theoretical graph (Fig 1B) is qualitatively comparable to the measured one (Fig 3C), we note quantitative disparities. For example, the local minima/maxima are separated approximately two times further in the experimental data than in the theoretical plot, and the sensitivity is diminished accordingly. Several factors contribute to this disparity. The theory assumes that the laser is positioned at the focus along the optical axis, and that the nanowire's translation direction is parallel to the focal plane. In practice these two conditions can only be met approximately. Additionally, the spotsize used in the theory is an estimate of the experimental conditions, based on the profile of the photodiode's sum signal. Finally, the SEM images in Fig 2B illustrate that our nanowires are not the perfect cylinders used in the model. Thus we use the theoretical predictions as rough guides for the expected sensitivity.

Thermal fluctuations establish the lower limit of force detection for the sensor. We measure the thermal motion of the nanowire by positioning it at the region of greatest sensitivity and detecting fluctuations in the difference signal of the split-photodiode. The sensitivity for this nanowire is linearly dependent upon the total incident laser power and was determined here to be $3.4\mu m/V$ (with $50\mu W$ incident) by a profile measurement such as Fig 3C. The bandwidth is determined by the transimpedence amplifiers, which is more than sufficient to detect the thermal oscillations of a $59\mu m$ long, 166nm radius nanowire, in air (e.g., Fig 3B).

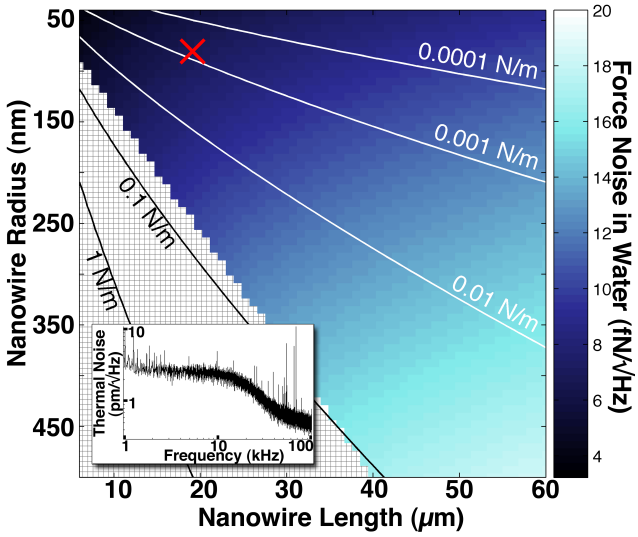

FIG. 4: The calculated[15] force-noises of nanowires as a function of their radii and lengths, in water. Contour lines denote cantilever stiffnesses, and the hashed region corresponds to thermal fluctuations that are too small to be detected with our system, with 5mW of laser power (see SI). Inset figure is the thermal of the $0.67mN/m$ stiff nanowire marked with a red X; its measured force noise in water is 1.9 $fN/\sqrt{Hz}$.

The position noise of a cantilever multiplied by its stiffness is its force noise, which is fundamentally determined from interactions between the cantilever and its surrounding fluid medium[15] (See Fig. 4). We immersed a nanowire 80nm in radius and 19.1 μm in length into water and used the 785nm laser to achieve a sensitivity of $0.5\mu m/V$ with 0.95mW of power. By multiplying its below-resonance position noise (2.84 $pm/\sqrt{Hz}$, see inset of Fig. 4) with its spring constant (0.67 mN/m), we determine its force noise to be 1.9 $fN/\sqrt{Hz}$. Currently, the best custom cantilevers we are aware of have force noises of 23-29$fN/\sqrt{Hz}$ in water [1, 16, 17] and commercial cantilevers have force-noises of 50-200 $fN/\sqrt{Hz}$[18].

We have shown that nanowires directionally scatter sufficient light to provide position detection with high sensitivity and bandwidth, without the need for an interferometric optical pathway. A split-photodiode sensor is sufficient to discern the changes in the Mie scattering of the nanowire as it moves across the focus of a beam. Our theoretical analysis indicates that for most nanowires the forwards scattering signal produces a significantly better sensitivity-to-noise ratio than backwards scattering. Moreover, the scheme is fully compatible with high damping environments, where it enables an order of magnitude or greater reduction in the force noise.

Currently, NEMS are limited by mechanisms to detect subtle displacements, particularly in ambient and fluid environments. The approach presented here addresses this shortcoming with an optical approach that is readily miniaturized and applicable to many geometries. With this method we achieve sub $pm/\sqrt{Hz}$ noise with high bandwidth, and have readily detected nanowires ranging from 72 to 451nm in radii. The approach enables significantly enhanced NEMS force sensors, and a dramatically lower fundamental force noise when performing AFM in high damping environments such as fluids.

Acknowledgments

We appreciate input from S. Aloni, V. Altoe, A.J. Katan, A. Muller-Egan, D.F. Ogletree, A.S. Risbud, M. Salmeron, P.J. Schuck, A.M. Schwartzberg, T.M. Short, A. Weber-Bargioni, and E. Wong. Work at the Molecular Foundry was supported by the Office of Science, Office of Basic Energy Sciences, of the U.S. Department of Energy under Contract No. DE-AC02-05CH11231.

[1] M. Viani, T. Schäffer, A. Chand, M. Rief, H. Gaub, and P. Hansma, Journal of Applied Physics **86**, 2258 (1999).
[2] D. Rugar, B. Stipe, H. Mamin, C. Yannoni, T. Stowe, K. Yasumura, and T. Kenny, Applied Physics A: Materials Science & Processing **72**, 3 (2001).
[3] K. Ekinci and M. Roukes, Review of Scientific Instruments **76**, 061101 (2005).
[4] B. Ilic, Y. Yang, and H. Craighead, Applied Physics Letters **85**, 2604 (2004).
[5] J. Nichol, E. Hemesath, L. Lauhon, and R. Budakian, Applied Physics Letters **93**, 193110 (2008).
[6] L. Biedermann, R. Tung, A. Raman, and R. Reifenberger, Nanotechnology **20**, 035702 (2009).
[7] M. Belov, N. Quitoriano, S. Sharma, W. Hiebert, T. Kamins, and S. Evoy, Journal of Applied Physics **103**, 074304 (2008).
[8] S. Kozaki, IEEE Transactions on Antennas and Propagation **30**, 881 (1982).
[9] S. Chavez-Cerda and G. New, Optics Communications **181**, 369 (2000).
[10] S. Kozaki, Journal of Applied Physics **53**, 7195 (1982).
[11] W. Gander and W. Gautschi, BIT Numerical Mathematics **40**, 84 (2000).
[12] F. Gittes and C. Schmidt, Optics letters **23**, 7 (1998).
[13] H. Kawakatsu, S. Kawai, D. Saya, M. Nagashio, D. Kobayashi, H. Toshiyoshi, and H. Fujita, Review of Scientific Instruments **73**, 2317 (2002).
[14] M. Yazdanpanah, S. Harfenist, A. Safir, and R. Cohn, Journal of Applied Physics **98**, 073510 (2005).
[15] J. Sader, Journal of applied physics **84**, 64 (1998).
[16] M. Antognozzi, A. Ulcinas, L. Picco, S. Simpson, P. Heard, M. Szczelkun, B. Brenner, and M. Miles, Nanotechnology **19**, 384002 (2008).
[17] A. Katan and T. Oosterkamp, The Journal of Physical Chemistry C **112**, 9769 (2008).
[18] *Asylum Research - The Olympus Bio-Lever.*

SI for: High sensitivity deflection detection of nano-cantilevers

Babak Sanii and Paul Ashby
Molecular Foundry, LBNL, Berkeley, CA 94618, USA
(Dated: 04 September 2009)

PACS numbers:

I. SENSITIVITY IN WATER

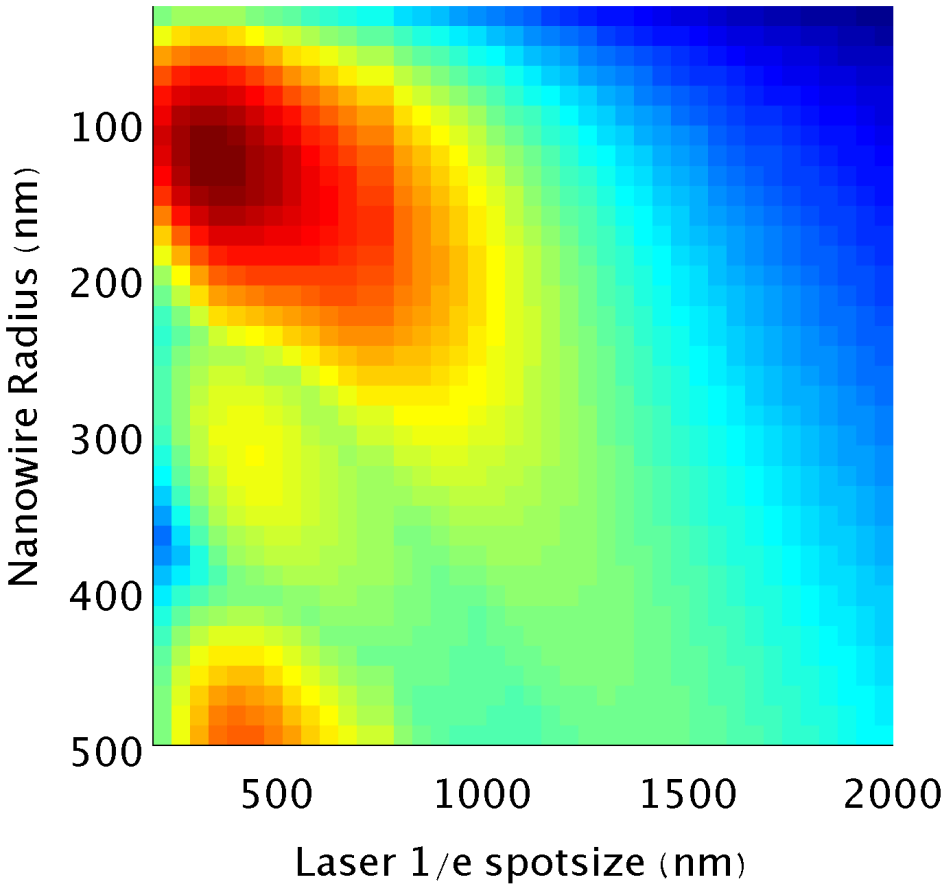

FIG. 1: A map of the sensitivity to noise ratio of the detection scheme in water as a function of 1/e spot diameter (39 samples, 200-2000nm) and nanowire radius (40 samples, 25-500nm), normalized and interpolated nearest-neighbor between samples. Sensitivity is defined as the steepest slope of the calculated translation profile (e.g., Fig 1B), and the relative noise is approximated by the square root of the total signal incident on the split photodiode.

II. DETERMINING MATERIAL PARAMETERS FROM THERMAL VIBRATION SPECTRA

The thermal fluctuation profile in Fig. 3B was fit with a Levenberg-Marquardt nonlinear regression[1] to a viscous fluid model of a cylindrical cantilever in air[2]. The physical dimensions of the nanowire cantilever were determined from SEM images (Fig. 2B) and nominal values for the density ($1.1778 km/m^3$) and viscosity ($1.8527 \times 10^{-5} Ns/m^2$) of air were used as fixed parameters of the fit. Our best-fit determines the density of the nanowire to be $7139.9 km/m^3$. We find the best-fit Young's modulus of 47.7GPa, which is within the previously measured range[3].

III. FORWARD SCATTERING VS. BACKWARD SCATTERING PLOTS

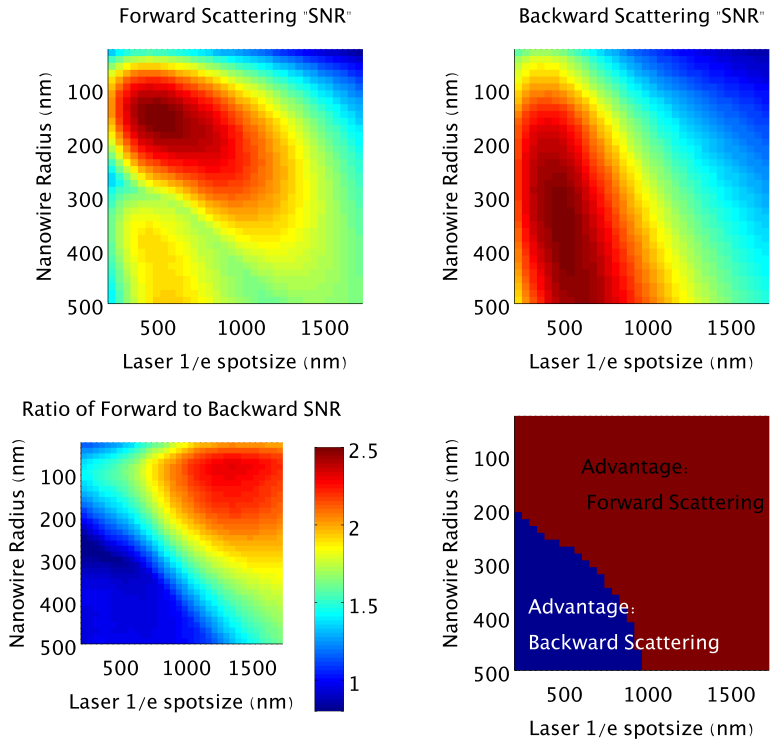

FIG. 2: Top-left: A map of the sensitivity to noise ratio of the detection scheme as a function of 1/e spot diameter (40 samples, 200-2000nm) and nanowire radius (40 samples, 25-500nm), normalized and interpolated nearest-neighbor between samples. Top-right: A similar plot looking at the backscatter signal. Bottom-left: The ratio of the forward to backward scattering. D: a map of where the ratio is greater than one (red region).

IV. DETERMINING WHEN NANOWIRE THERMAL FLUCTUATIONS IN WATER ARE DETECTABLE BY OUR SYSTEM

With a fixed amount of input laser power, there is a limit to the smallest nanowire movement we can detect. This corresponds to the a range of nanowire sizes whose thermal fluctuations we can discern. We calculated this by normalizing the theoretical sensitivity in water with a measured sensitivity point (shown on the graph with a red X, radius = 80nm,length = 19.1 μm), scaling it to 5mW of detected power (accounting for backscattering losses from the nanowire), and considering only the spotsize of that experiment ($\approx 1650nm$). The shot noise is considered in addition to the input noise of the Asylum Controller (300 $nV/\sqrt{Hz}$). In this way an expected noise floor as a function of nanowire radius was determined.

Next, we calculated the thermal fluctuations in water of a range of nanowire radii and lengths per Sader's viscous model[2] and compared the off-resonance thermal fluctuation amplitude with the expected noise floor. The hashed region in figure 4 is where the noise floor is greater than the expected thermal fluctuations. We note that increased laser power expands the range of accessible nanowires. Preliminary results indicate that the ultimate limit may be the onset of heating damage of the nanowire or boiling of the surrounding water.

[1] Y. Bard, *Nonlinear parameter estimation* (Academic Press New York, 1974).
[2] J. Sader, Journal of applied physics **84**, 64 (1998).
[3] M. Yazdanpanah, Ph.D. thesis, University of Louisville (2006).